



저작자표시-비영리-변경금지 2.0 대한민국

이용자는 아래의 조건을 따르는 경우에 한하여 자유롭게

- 이 저작물을 복제, 배포, 전송, 전시, 공연 및 방송할 수 있습니다.

다음과 같은 조건을 따라야 합니다:



저작자표시. 귀하는 원저작자를 표시하여야 합니다.



비영리. 귀하는 이 저작물을 영리 목적으로 이용할 수 없습니다.



변경금지. 귀하는 이 저작물을 개작, 변형 또는 가공할 수 없습니다.

- 귀하는, 이 저작물의 재이용이나 배포의 경우, 이 저작물에 적용된 이용허락조건을 명확하게 나타내어야 합니다.
- 저작권자로부터 별도의 허가를 받으면 이러한 조건들은 적용되지 않습니다.

저작권법에 따른 이용자의 권리는 위의 내용에 의하여 영향을 받지 않습니다.

이것은 [이용허락규약\(Legal Code\)](#)을 이해하기 쉽게 요약한 것입니다.

[Disclaimer](#)

Abstract

A Rational Design of Suzuki–Miyaura Catalyst–Transfer Polycondensation: Marriage of Palladacycle Precatalysts with MIDA–boronates

Kyeong–Bae Seo
Department of Chemistry
(Organic Chemistry)
The Graduate School
Seoul National University

Herein, we report a highly efficient Suzuki–Miyaura catalyst–transfer polycondensation (SCTP) of 3–alkylthiophenes using bench–stable but highly active Buchwald dialkylbiarylphospine Pd G3 precatalysts and *N*–methylimidodiacetic (MIDA)–boronate monomers. Initially, the feasibility of the catalyst–transfer process was examined by screening various dialkylbiarylphospine–Pd(0) species. After optimizing a small molecule model reaction, we identified both RuPhos and SPhos Pd G3 precatalysts as excellent catalyst systems for this purpose. Based on these model studies, SCTP was tested using either RuPhos or SPhos Pd G3 precatalyst, and 5–bromo–4–*n*–hexylthien–2–yl–pinacol–boronate. Poly(3–hexylthiophene) (P3HT) was produced with controlled molecular weight and narrow dispersity for a low degree of polymerization (DP) only, while attempts to synthesize P3HT having a higher DP with

good control were unsuccessful. To improve the control, slowly hydrolyzed 5-bromo-4-*n*-hexylthien-2-yl-MIDA-boronate was introduced as a new monomer. As a result, P3HT and P3EHT (up to 20 kg/mol) were prepared with excellent control, narrow dispersity, and excellent yield (>90 %). Detailed mechanistic investigation using ³¹P NMR and MALDI-TOF revealed that both fast initiation using Buchwald precatalysts and the suppression of protodeboronation due to the protected MIDA-boronate were crucial to achieve successful living polymerization of P3HT. In addition, a block copolymer of P3HT-*b*-P3EHT was prepared via SCTP by sequential addition of each MIDA-boronate monomer. Furthermore, the same block copolymer was synthesized by one-shot copolymerization for the first time by using fast propagating pinacol-boronate and slow propagating MIDA-boronate. Finally, this one-shot block copolymerization strategy led to the highly efficient and direct *in situ* production of star polythiophenes.

Keywords: Suzuki-Miyaura catalyst-transfer polycondensation, Poly(3-alkylthiophene), Buchwald precatalyst, MIDA-boronates, One-shot polymerization, *In situ* nanoparticlization of conjugated polymer.

Student Number: 2015-20384

Contents

Abstract	1
Contents	3

A Rational Design of Suzuki–Miyaura Catalyst–Transfer Polycondensation: Marriage of Palladacycle Precatalysts with MIDA–boronates

Introduction	4
Experimental	8
Results and Discussion	18
Conclusions	37
Reference	38

Abstract (Korean)	41
-------------------	----

Introduction

Conjugated polymers have attracted much attention amongst chemists because their intriguing applications to optoelectronic devices have provided promising technological advantages such as solution processibility, flexibility, low cost, and tunability of optoelectronic properties.¹ For example, poly(3-hexylthiophene) (P3HT) is one of the most extensively studied conjugated polymers in polymer electronics due to its good solubility, excellent thermal stability, and high hole mobility.² In line with an increasing interest in polymer electronics, the importance of developing new synthetic methodologies to prepare novel conjugated polymers has also grown over the past two decades. Conventionally, most of these conjugated polymers were prepared by a step-growth polymerization method using coupling reactions such as the Suzuki, Stille, and Heck reactions.³ While these methods produced conjugated polymers with well-defined conjugated backbones, the precise control of their molecular weights, polydispersity index (PDI), and chain-ends was virtually impossible. In contrast to step-growth polymerization, controlled chain-growth polymerization methods provide conjugated polymers with precise control, thereby allowing facile access to various functional materials such as block copolymers, complex macromolecular architecture (e. g. graft copolymers), and hybrid nanomaterials modified with conjugated polymers.⁴ Therefore, developing new controlled chain-growth polymerization methods for the synthesis of conjugated polymers has been one of the main focuses in

polymer chemistry. For example, pioneering works on the Kumada catalyst-transfer polycondensation (KCTP) method, the most widely used CTP method, provided a breakthrough in the synthesis of various conjugated polymers including P3HT and their corresponding block copolymers.⁵ However, despite the versatility of KCTP, the use of stoichiometric amounts of moisture-sensitive and reactive Grignard reagents often limited the molecular weight control, yield, potential monomer scope, and synthetic applications (Figure 1a). Moreover, preparation of externally initiated nickel catalysts required multiple synthetic steps or glove box techniques.⁶ Therefore, to overcome these issues, the Suzuki-Miyaura reaction, using air and moisture stable boronates, has emerged as a promising alternative for CTP.⁷

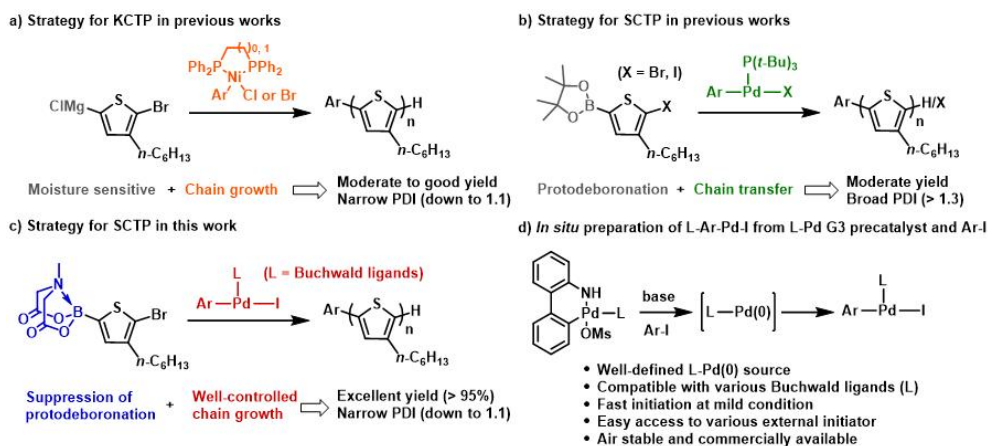


Figure 1. Strategies for the controlled chain-growth polymerization of P3HT using (a) KCTP and (b) SCTP methods in previous works; (c) our strategy using L-Pd G3 precatalysts and MIDA-boronates for SCTP of 3HT; and (d) preparation of externally initiated catalysts.

Suzuki-Miyaura reaction has attracted growing academic and industrial interest because its synthetic advantages based on mild

reaction conditions, broad substrate scope, high functional group tolerance, and non-toxic monomers, particularly which are a sharp contrast to analogous Stille reaction requiring toxic tin compounds, have been overwhelming for synthesizing both small molecules and macromolecules.⁸⁻¹⁰ Indeed, huge efforts have been devoted to fine-tuning the structures of palladium (Pd)-ligands and boronates to develop milder, more efficient, and versatile Suzuki-Miyaura reactions.^{8,9} While there has been remarkable progress in Suzuki-Miyaura coupling reactions as popular organic reactions and step-growth polymerization methods,⁸⁻¹⁰ to date, the controlled chain-growth polymerization of 3-alkylthiophenes (P3AT) using Suzuki-Miyaura catalyst-transfer polycondensation (SCTP) is still challenging. This is mainly because of the use of a less efficient catalyst system and the competing protodeboronation of heterocyclic boronate monomers (Figure 1b). For example, SCTP of 3-hexylthiophene containing a pinacol boronic ester, using well-defined $P(t\text{-Bu})_3\text{-Pd-Ph-Br}$ or Pd-containing *N*-heterocycliccarbenes, produced P3HT with a broad PDI (>1.3), moderate yields, and mixed chain-ends due to competing protodeboronation.¹¹ As a result, well-defined block copolymers containing both polythiophene moieties have not been demonstrated. Therefore, even though the SCTP method exhibited many advantages over KCTP, its overall efficiency as the controlled polymerization of P3AT was less than satisfactory, thereby prohibiting the wide use of SCTP for P3AT synthesis. Thus, given the importance of P3AT with its wide range of applications, developing a more efficient SCTP method that achieves both excellent controllability and productivity would be highly desirable.

Herein, we report a breakthrough on the controlled chain-growth polymerization of 3-alkylthiophenes via a catalyst-transfer process using highly active, fast initiating, and bench-stable Buchwald

palladacycle precatalysts and *N*-methylimidodiacetic (MIDA) boronate protection to suppress protodeboronation (Figure 1c). As a result of these two modifications, SCTP of P3AT proceeded with excellent control on molecular weight and chain-ends, narrow PDI, excellent regioregularity, and quantitative conversion. Moreover, for the first time, the utility of this highly controlled polymerization protocol was expanded to successful block copolymerization of fully conjugated diblock copolymers comprising both polythiophene moieties, even in one-shot copolymerization. Lastly, the power of the new SCTP protocol over the widely used KCTP method was further demonstrated by another one-shot block copolymerization to produce semi-conducting polythiophene star polymers via direct *in situ* self-assembly.

Experimental

Materials

Unless otherwise noted, all reagents were purchased from commercial sources and used without further purification. Tetrahydrofuran (THF) was distilled over sodium and benzophenone, and degassed by argon bubbling for 10 minutes before using on polymerization. 5-Bromo-4-*n*-hexylthien-2-yl-pinacol-boronate (**M3**) and 5-bromo-4-*n*-hexylthien-2-yl-MIDA-boronate (**M4**) were prepared by previously reported procedures.^{10b} 5-Bromothien-2-yl-MIDA-boronate (**M7**) was prepared by previously reported procedure.^{9a}

General analytical information

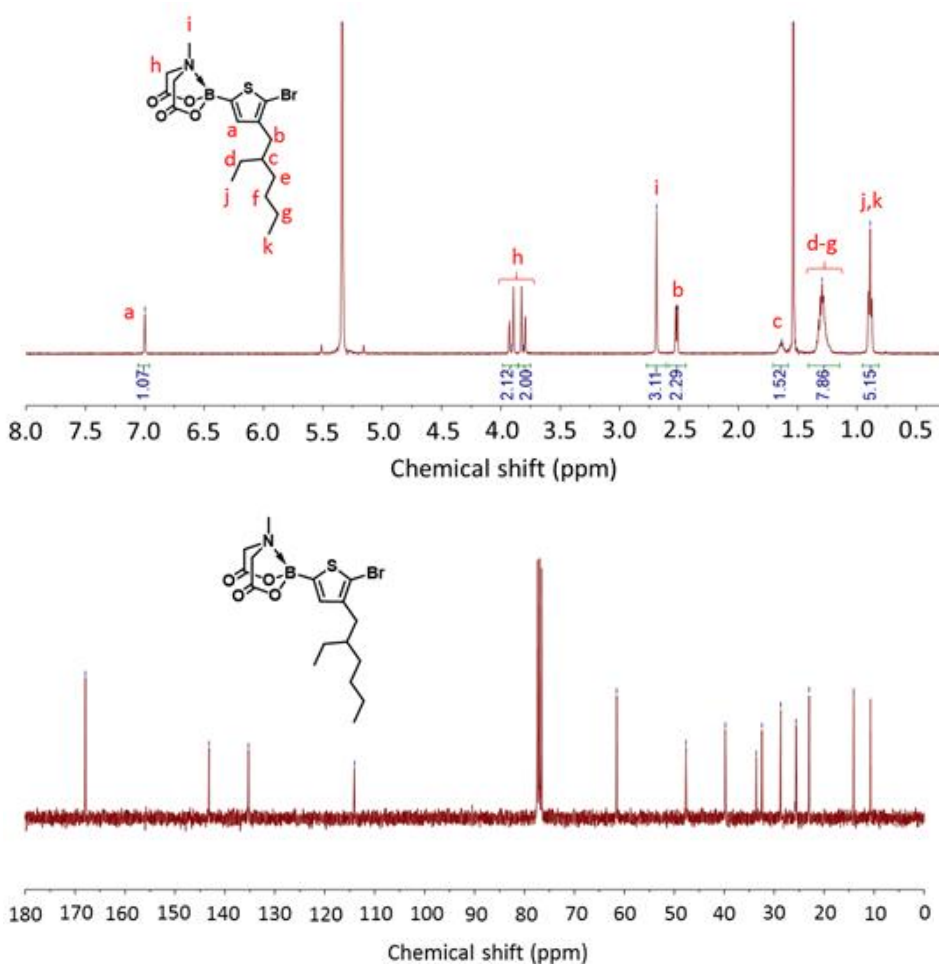
NMR spectra were recorded by Varian/Oxford As-500 (500 MHz for ¹H) and Agilent 400-MRDD2 Magnetic Resonance System (400 MHz for ¹H, 162 MHz for ³¹P) spectrometers. THF Size exclusion chromatography (SEC) for polymer molecular weight analysis was carried out with Waters system (1515 pump, 2414 refractive index detector and 2489 UV detector) and Shodex SEC LF-804 column eluted with THF (SEC grade, Honeywell Burdick & Jackson). Flow rate was 1.0 mL/min and temperature of the column was maintained at 35 °C. Samples were diluted in 0.001-0.005 wt% by THF and filtered through a 0.20 μm PTFE filter before injection into the SEC. The molar masses of macromonomers were measured by Bruker Daltonics autoflex II TOF/TOF. Dithranol in THF was used as a matrix. UV/Vis spectra were obtained by Jasco Inc. UV/vis Spectrometer V-550. Dynamic light scattering (DLS) data were obtained by Malvern Zetasizer Nano ZS. Multimode 8 and Nanoscope

V controller (Veeco Instrument) were used for atomic force microscopy (AFM) imaging. Transmission electron microscopy (TEM) imaging was performed by using JEM-2100 (JEOL) at 120 kV.

Procedures for the preparation of monomers

(a) 5-Bromo-4-(2-ethylhexyl)thien-2-yl-MIDA-boronate (**M5**)

M5 was prepared by the slightly modified method from the previous literature.^{10b}

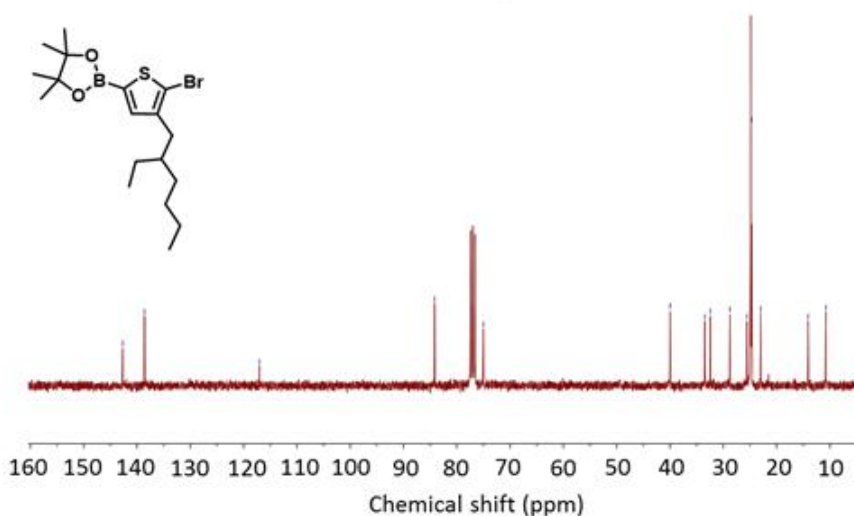
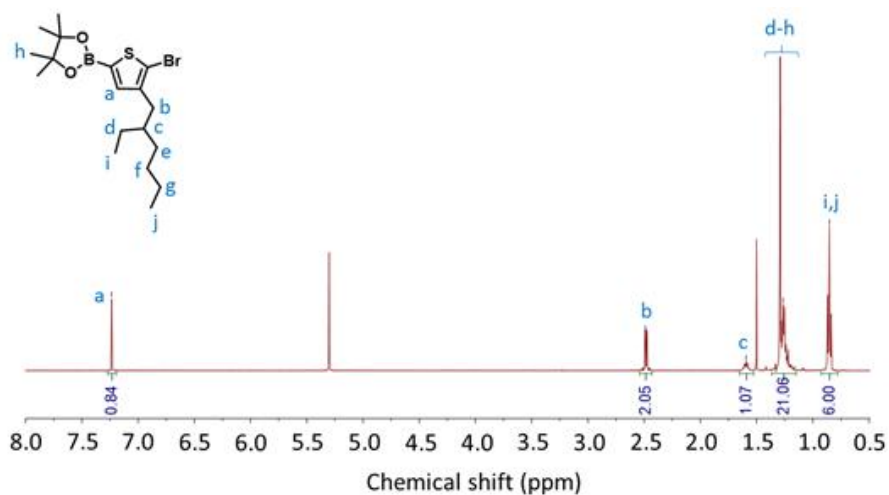


¹H NMR (500 MHz, CD₂Cl₂) δ7.00 (s, 1H), 3.91 (dd, *J* = 16.5, 2.0 Hz,

2H), 3.81 (dd, $J = 16.5, 2.1$ Hz, 2H), 2.69 (d, $J = 1.9$ Hz, 3H), 2.52 (d, $J = 7.2$ Hz, 2H), 1.61 (d, $J = 31.3$ Hz, 1H), 1.30 (dd, $J = 13.8, 6.4$ Hz, 8H), 0.89 (t, $J = 7.4$ Hz, 6H).¹³ C NMR (75 MHz, CDCl₃) δ 167.93, 143.19, 135.28, 114.05, 61.55, 47.68, 39.80, 33.60, 32.47, 28.68, 25.6, 23.00, 14.09, 10.74. ESI MS calculated for [M+Na]⁺452.0676, found 452.0678.

(b) 5-Bromo-4-(2-ethylhexyl)thien-2-yl-pinacol-boronate (**M6**)

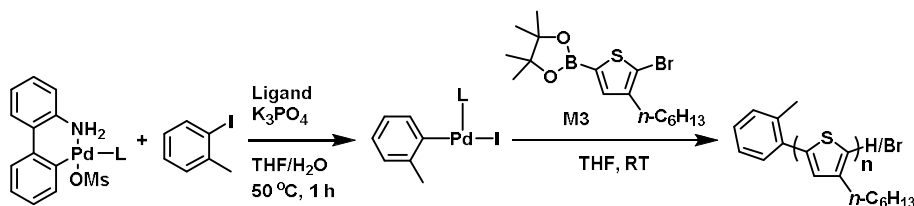
M6 was prepared by the slightly modified method from the previous literature.^{10b}



^1H NMR (500 MHz, CD_2Cl_2) δ 7.24 (s, 1H), 2.48 (dd, $J=7.2, 1.7$ Hz, 2H), 1.66 - 1.54 (m, 1H), 1.35 - 1.16 (m, 20H), 0.86 (td, $J = 7.2, 2.3$ Hz, 6H). ^{13}C NMR (75 MHz, CDCl_3) δ 142.68, 138.58, 117.04, 84.18, 74.99, 39.97, 33.44, 32.44, 28.74, 25.53, 24.81, 22.98, 14.08, 10.74. ESI MS calculated for $[\text{M}+\text{Na}]^+$ 423.1139, found 423.1140.

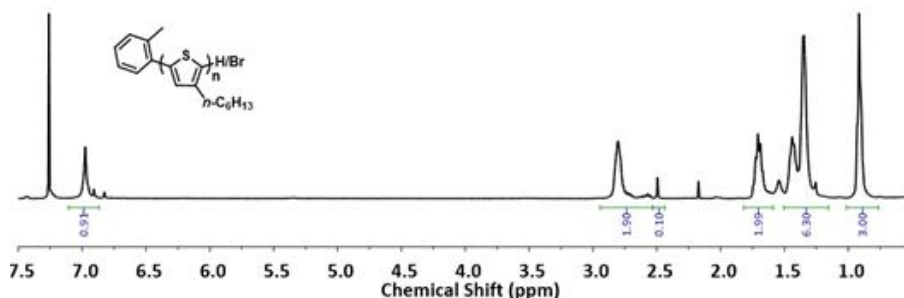
General polymerization procedures

(a) Synthesis of P3HT from M3

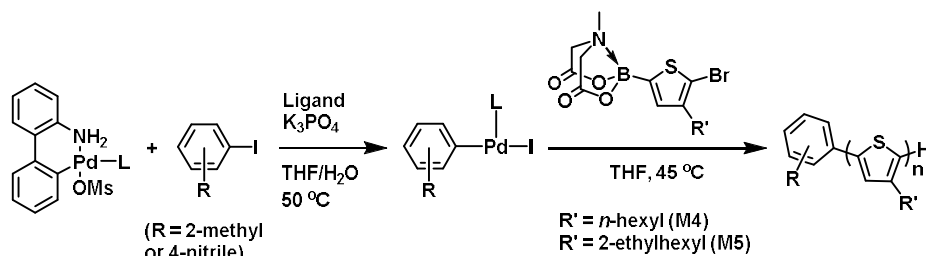


To a round-bottom flask equipped with stir bar, Buchwald G3 precatalyst (0.008 mmol), 2-iodotoluene (0.0076 mmol), ligand (0.012 mmol), and K_3PO_4 (1.2 mmol) were added. The flask was evacuated and backfilled with argon three times. Degassed THF (2 mL) and H_2O (0.3 mL) were then added. The mixture was heated and stirred at 50 °C for 1 h to prepare externally initiated catalyst. M3 (0.2 mmol where $\text{M}/\text{I} = 25/1$) in degassed THF (12 mL) was then added to the flask, and the polymerization was left to stir at room temperature for 14-24h. The polymerization was quenched with 6 N HCl solution (5 mL). The crude reaction mixture was diluted with CHCl_3 , washed with brine, dried over anhydrous MgSO_4 , and concentrated under reduced pressure. The polymer was purified by precipitation into methanol. The precipitate was collected by filtration, washed with methanol, and dried under vacuum.

^1H NMR spectrum of P3HT from **M3**



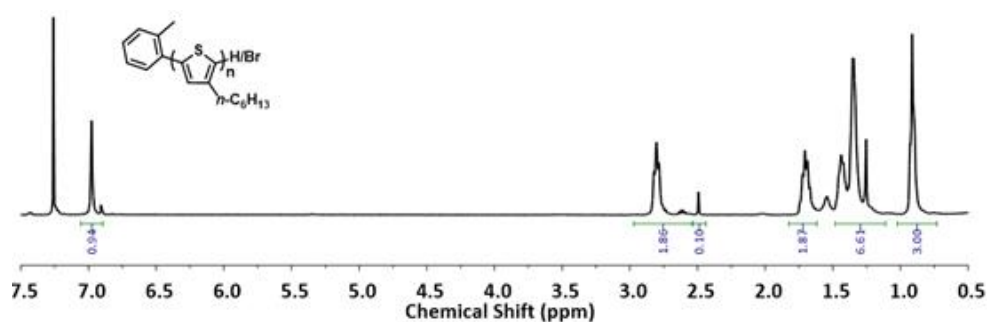
(b) Synthesis of P3AT from **M4** (or **M5**)



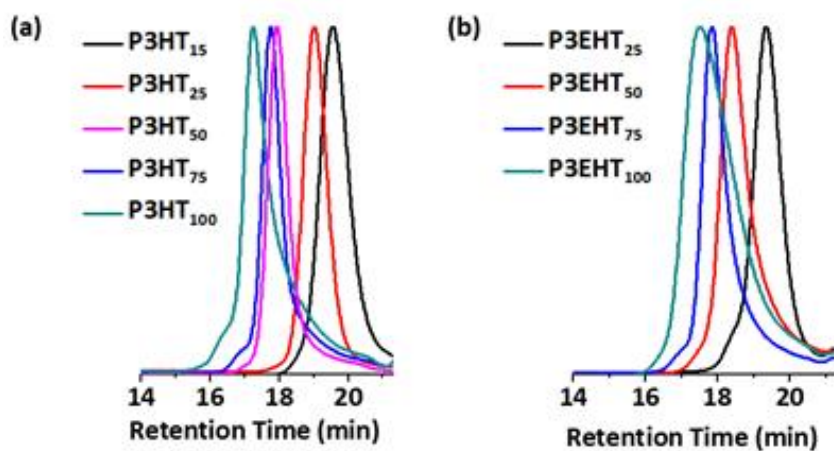
To a round-bottom flask equipped with stir bar, Buchwald G3 precatalyst (0.008 mmol), aryl iodide (0.0076 mmol), ligand (0.012 mmol), and K_3PO_4 (1.2 mmol) were added. The flask was evacuated and backfilled with argon three times. Degassed THF (2 mL) and H_2O (0.72 mL) were then added. The mixture was heated and stirred at 50 °C for 15 minutes (for 4-iodobenzonitrile) or 1 h (for 2-iodotoluene) to prepare externally initiated catalyst. **M4** or **M5** (0.2 mmol where M/I = 25/1) in degassed THF (17 mL) was then added to the flask, and the polymerization was left to stir at 45 °C for 15–25h. The polymerization was quenched with 6 N HCl solution (5 mL). The crude reaction mixture was diluted with CHCl_3 , washed with brine, dried over anhydrous MgSO_4 , and concentrated under reduced pressure. The

polymer was purified by precipitation into methanol. The precipitate was collected by filtration, washed with methanol, and dried under vacuum.

^1H NMR spectrum of P3HT from M4

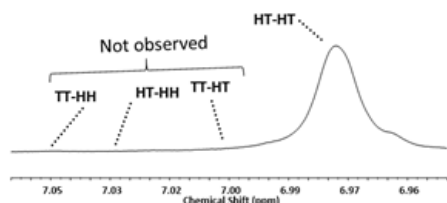


SEC RI traces of (a) P3HT and (b) P3EHT (eluent: THF)

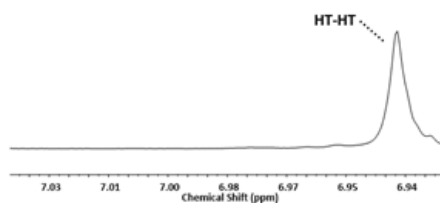


^1H NMR spectra of (a) P3HT and (b) P3EHT showing $\sim 100\%$ regioregularity^{11a}

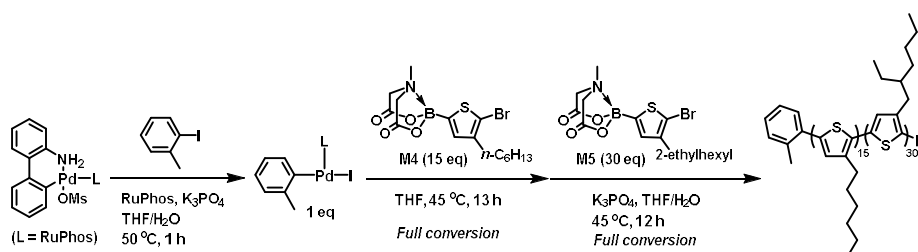
(a) P3HT



(b) P3EHT



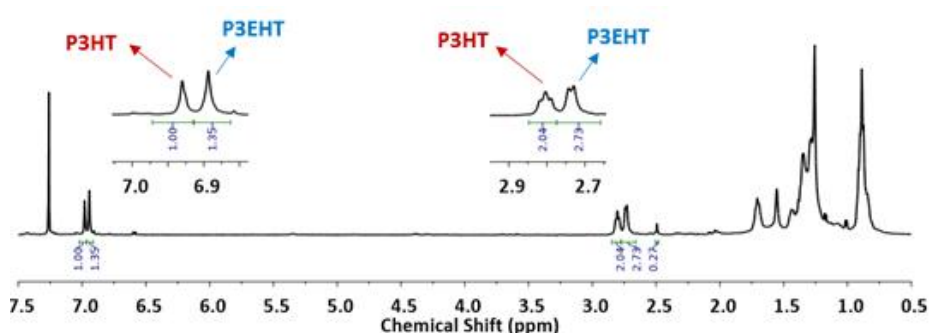
(c) Synthesis of P3HT-*b*-P3EHT block copolymer by sequential monomer addition (**M4** followed by **M5**)



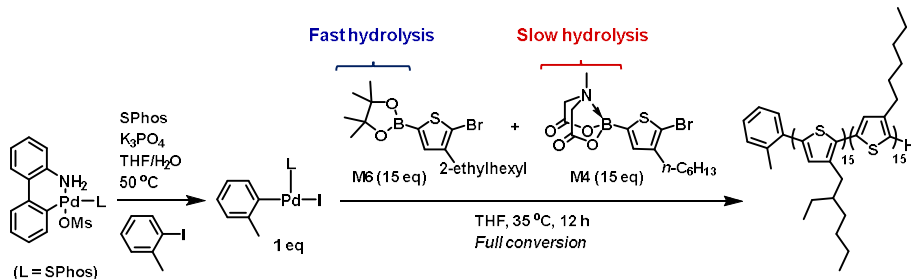
To a round-bottom flask equipped with stir bar, RuPhos G3 precatalyst (0.0133 mmol), 2-iodotoluene (0.0127 mmol), RuPhos (0.020 mmol), and K₃PO₄ (1.2 mmol) were added. The flask was evacuated and backfilled with argon three times. Degassed THF (2 mL) and H₂O (0.72 mL) were then added. The mixture was heated and stirred at 50 °C for 15 minutes to prepare externally initiated catalyst. **M4** (0.2 mmol) in degassed THF (19 mL) was then added to the flask, and the polymerization was left to stir at 45 °C for 13 h. Subsequently, **M5** (0.4 mmol) in degassed THF (20 mL) and K₃PO₄ (1.2 mmol) in degassed H₂O (0.72 mL) were added to the flask, and the polymerization was left to stir at 45 °C for 12 h. The polymerization was quenched with 6 N HCl solution (5 mL). The crude reaction mixture was diluted with CHCl₃, washed with brine, dried over anhydrous MgSO₄, and concentrated under reduced pressure. The polymer was purified by

precipitation into methanol. The precipitate was collected by filtration, washed with methanol, and dried under vacuum (84 mg, 75 %).

^1H NMR spectrum of P3HT-*b*-P3EHT



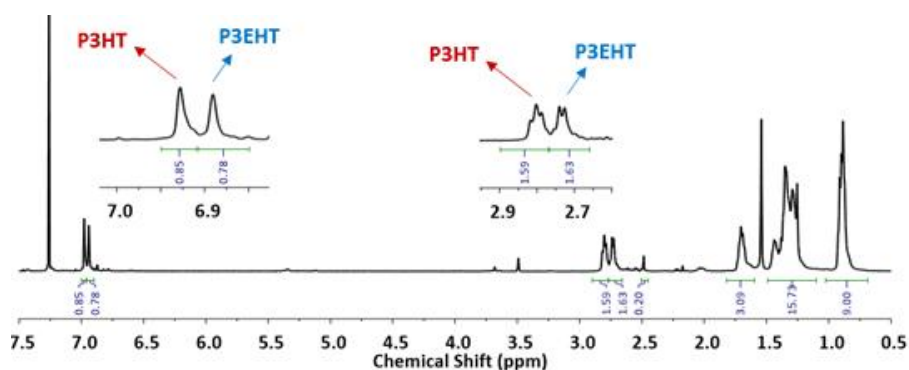
(d) Synthesis of P3EHT-*b*-P3HT block copolymer by simultaneous monomer addition



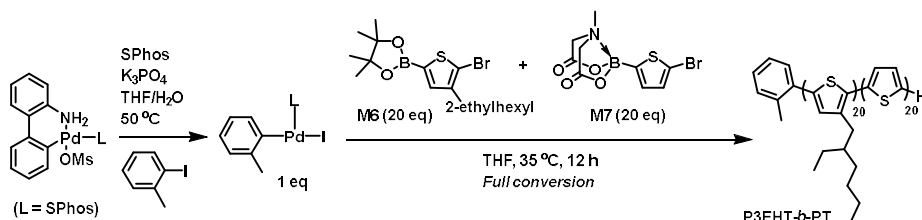
To a round-bottom flask equipped with stir bar, SPhos G3 precatalyst (0.0133 mmol), 2-iodotoluene (0.0127 mmol), SPhos (0.020 mmol), and K_3PO_4 (1.2 mmol) were added. The flask was evacuated and backfilled with argon three times. Degassed THF (2 mL) and H_2O (0.6 mL) were then added. The mixture was heated and stirred at 50 °C for 1 h to prepare externally initiated catalyst. **M4** (0.1 mmol) and **M6** (0.1 mmol) in degassed THF (10 mL) were then added to the flask, and the polymerization was left to stir at 35 °C for 12 h. The

polymerization was quenched with 6 *N* HCl solution (5 mL). The crude reaction mixture was diluted with CHCl₃, washed with brine, dried over anhydrous MgSO₄, and concentrated under reduced pressure. The polymer was purified by precipitation into methanol. The precipitate was collected by filtration, washed with methanol, and dried under vacuum (30 mg, 83 %).

¹H NMR spectrum of P3EHT-*b*-P3HT



(e) Synthesis of P3EHT-*b*-PT block copolymer by simultaneous monomer addition



To a round-bottom flask equipped with stir bar, SPhos G3 precatalyst (0.01 mmol), 2-iodotoluene (0.0095 mmol), SPhos (0.015 mmol), and K₃PO₄ (1.2 mmol) were added. The flask was evacuated and backfilled with argon three times. Degassed THF (2 mL) and H₂O (0.6 mL) were then added. The mixture was heated and stirred at 50 °C for 1 h to prepare externally initiated catalyst. **M6** (0.1 mmol) and **M7** (0.1

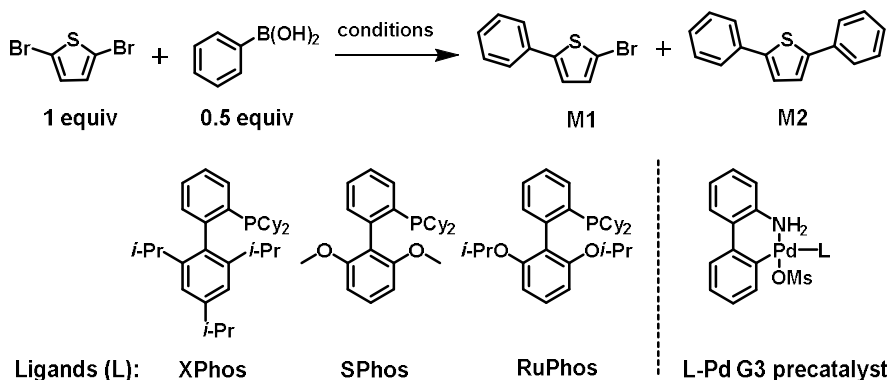
mmol) in degassed THF (10 mL) were then added to the flask, and the polymerization was left to stir at 35 °C for 12 h. The polymerization was quenched with 6 *N* HCl solution (5 mL). The crude reaction mixture was diluted with CHCl₃, washed with brine, dried over anhydrous MgSO₄, and concentrated under reduced pressure. The polymer was purified by precipitation into methanol. The precipitate was collected by filtration, washed with methanol, and dried under vacuum (22 mg, 78 %).

Results and Discussion

Pd-catalyzed Suzuki–Miyaura coupling of aryl halides and aryl boronic acids is one of the most versatile, efficient, and widely used reactions employed to construct biaryl moieties; thus, numerous efforts have been made to develop more powerful catalyst systems.⁸ Among them, dialkylbiarylphosphine ligand–Pd(0) (L–Pd(0)) species, commonly known as Buchwald catalysts, are one of the most popular catalysts in the Suzuki–Miyaura reaction not only because they are highly active, stable, and user-friendly, but also because many variants are commercially available for easy optimization screening.^{8e–i} Interestingly, despite the versatility of the Buchwald L–Pd(0) system in cross-coupling reactions, its catalyst-transfer process, which could potentially lead to SCTP, has not been demonstrated to date. Therefore, to investigate the possibility of a catalyst-transfer process by L–Pd(0), we carried out some model studies by conducting small molecule Suzuki–Miyaura reactions of 2,5-dibromothiophene (1 equiv.) and phenylboronic acid (0.5 equiv., Table 1).

A substoichiometric amount of phenylboronic acid was intentionally employed in the model reaction. In this way, analysis of product distribution of mono-functionalized 2-bromo-5-phenylthiophene (**M1**) and di-functionalized 2,5-diphenylthiophene (**M2**) would demonstrate the degree of the catalyst-transfer process by various L–Pd(0) systems (Table 1).^{11c} In more detail, conventional statistics would favor the formation of **M1** over **M2** in the absence of a catalyst-transfer process. However, if the Pd catalyst undergoes intramolecular oxidative addition via the catalyst-transfer process, **M2**

Table 1. Screening of the catalyst-transfer process in small molecule reaction using Pd(0)/ligands and Pd G3 precatalysts

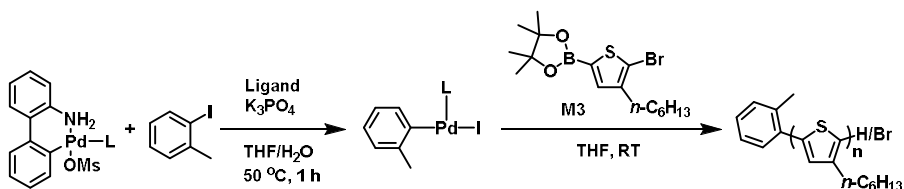


Entry	Pd catalyst (equiv.)	Ligand (equiv.)	THF/H ₂ O (conc., v/v)	Molar ratio (M1:M2)
1	Pd ₂ dba ₃ (0.02)	none	0.4 M, 2/1	70:30
2	Pd ₂ dba ₃ (0.02)	XPhos (0.04)	0.4 M, 2/1	39:61
3	Pd ₂ dba ₃ (0.02)	XPhos (0.08)	0.4 M, 2/1	15:85
4	Pd ₂ dba ₃ (0.02)	XPhos (0.08)	0.03 M, 30/1	6:94
5	Pd ₂ dba ₃ (0.02)	SPhos (0.08)	0.03 M, 30/1	4:96
6	Pd ₂ dba ₃ (0.02)	RuPhos (0.08)	0.03 M, 30/1	4:96
7	SPhos Pd G3 (0.04)	SPhos (0.04)	0.03 M, 30/1	2:98
8	RuPhos Pd G3 (0.04)	RuPhos (0.04)	0.03 M, 30/1	2:98

Reaction conditions: 2,5-dibromothiophene (0.2 mmol), phenylboronic acid (0.1 mmol), K₃PO₄ (1.2 mmol), THF / H₂O (12 mL / 0.4 mL for 0.03 M), room temperature, overnight. Molar ratio and yield were determined by gas chromatography-massspectrometry (GC-MS) calibrated using undecane as a standard.

should be dominantly produced over **M1**. To investigate the possibility of the catalyst-transfer process, the small molecule model reaction was initially performed using tris(dibenzylideneacetone)dipalladium(0) (Pd_2dba_3 ; 0.02 equiv.) in THF/ H_2O (0.4 M, v/v = 2/1) at room temperature as a control experiment. As expected, **M1** was preferentially produced over **M2** (**M1:M2** = 70:30) (Table 1, entry 1). In contrast, adding one equiv. of 2-dicyclohexylphosphino-2',4',6'-triisopropylbiphenyl (XPhos) ([Pd]:[XPhos] = 1:1) to the reaction switched the preference from **M1** to **M2** (**M1:M2** = 39:61), implying a partial catalyst-transfer process (Table 1, entry 2). To enhance this effect, the amount of XPhos ligand was doubled ([Pd]:[XPhos] = 1:2) and the preference of **M2** further increased (**M1:M2** = 15:85) (Table 1, entry 3). To push the selectivity for **M2** over to **M1**, the reaction was performed in dilute conditions to further promote the intramolecular catalyst-transfer process (0.03 M, THF/ H_2O (v/v) = 30/1) and indeed, the preference improved significantly (**M1:M2** = 6:94; Table 1, entry 4). With these results in hand, we subsequently tested other Buchwald ligands such as 2-dicyclohexylphosphino-2',6'-dimethoxybiphenyl (SPhos) and 2-dicyclohexylphosphino-2',6'-diisopropoxybiphenyl (RuPhos) and found that in both cases, the selectivity for **M2** increased further (**M1:M2** = 4:96; Table 1, entries 5 and 6). Finally, we observed that commercially available SPhos Pd G3 and RuPhos Pd G3 precatalysts were the best choices, affording the highest selectivity (**M1:M2** = 2:98). This was probably attributed to more efficient formation of the active Pd(0) catalysts (Table 1, entries 7 and 8).⁸ⁱ In short, excellent catalyst-transfer of XPhos-Pd(0), SPhos-Pd(0), and RuPhos-Pd(0) in the Suzuki-Miyaura reaction was realized.

Table 2. Screening of SCTP using M3 and various Pd catalysts



Entry	M/I	Pd catalyst (equiv.)	Ligand (equiv.)	THF/H ₂ O (conc., v/v)	Time	M _n (PDI) ^a	Yield ^b
1	25	Pd ₂ dba ₃ (0.02)	SPhos (0.10)	0.02 M, 40/1	14 h	10.2k (1.70)	64%
2	25	SPhos Pd G3 (0.04)	none	0.02 M, 40/1	24 h	6.6k (1.47)	85%
3	25	SPhos Pd G3 (0.04)	SPhos (0.06)	0.02 M, 40/1	21 h	6.6k (1.21)	82%
4	25	RuPhos Pd G3 (0.04)	RuPhos (0.06)	0.02 M, 40/1	21 h	5.2k (1.19)	78%
5	25	XPhos Pd G3 (0.04)	XPhos (0.06)	0.02 M, 40/1	14 h	5.7k (1.64)	62%
6	25	P(<i>t</i> -Bu) ₃ Pd G3 (0.04)	P(<i>t</i> -Bu) ₃ (0.06)	0.02 M, 40/1	16 h	7.6k (1.48)	81%
7	50	SPhos Pd G3 (0.02)	SPhos (0.03)	0.02 M, 40/1	16 h	9.8k (1.39)	64%
8	50	RuPhos Pd G3 (0.02)	RuPhos (0.03)	0.02 M, 40/1	16 h	11.8k (1.66)	60%

Reaction conditions: **M3**(0.2mmol,1 equiv.), Pd G3 precatalyst, ligand, K₃PO₄ (1.2 mmol), THF (12 mL), H₂O (0.3 mL), room temperature. ^aTHF SEC calibrated using polystyrene standards. ^bIsolated yield.

After successful demonstration of the catalyst-transfer of L-Pd(0) in small molecule model studies (Table 1), we moved on to develop a new controlled chain-growth polymerization method (Table 2). Synthesis of P3HT was selected as the model polymerization because not only it was widely used in polymer electronics but also its previous examples of controlled polymerization, using the SCTP method, exhibited some limitations such as broad PDI and moderate polymerization yields (Figure 1b).¹¹ As an initial trial, we carried out the polymerization of 5-bromo-4-*n*-hexylthien-2-yl-pinacol-boronate

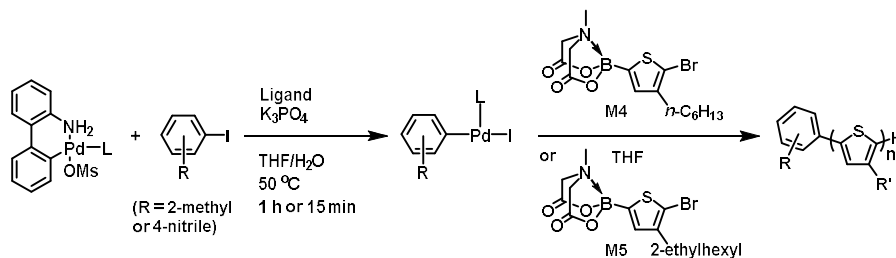
(**M3**) using a catalyst system of Pd₂dba₃, SPhos, and 2-iodotoluene (**M3**: $[Pd]$ = 25:1) in THF/H₂O mixed solvents (0.02 M, v/v = 40/1) at room temperature (Table 2, entry 1). Disappointingly, polymerization of **M3** afforded P3HT with an excessively large M_n value of 10.2 kg/mol, broad PDI of 1.70, and 64 % isolated yield in 14 h (Table 2, entry 1). This implied that despite the catalyst-transfer process of SPhos-Pd(0), the initiation must have been very slow, presumably due to the inefficient formation of the externally initiated SPhos-Pd(II)-(o-tolyl)-I catalyst. Thus, to attain fast initiation, 2-iodotoluene and a well-defined SPhos Pd G3 precatalyst, known to rapidly form active Pd(0), were used instead to efficiently generate the actual initiator (Table 2, entry 2).⁸ⁱ Indeed, switching to the precatalyst afforded better polymerization control, yielding P3HT with a relatively narrower PDI (1.47) and a molecular weight that was closer to the theoretical value (M_{theo} = 4.3 kg/mol). This confirmed the importance of Pd sources towards the initiation process (Table 2, entry 2). Encouraged by this significant improvement, we further optimized the polymerization conditions by adding another 0.06 equiv. of SPhos ligands during the catalyst preparation step to increase the stability of the catalysts attached at the polymer chain-end and to facilitate the catalyst-transfer process (Table 2, entry 3). Notably, the addition of an extra amount of SPhos ligand further improved the polymerization control by reducing the PDI to 1.21 (Table 2, entry 3). Using these conditions, we screened other G3 precatalyst derivatives containing RuPhos, XPhos, and P(*t*-Bu)₃. We discovered that only the RuPhos G3 precatalyst led to excellent controlled polymerization, affording P3HT with M_n of 5.2 kg/mol and narrow PDI of 1.19 in 78% yield (Table 2, entry 4). Disappointingly, poor control (PDI = 1.64) was observed with the XPhos Pd G3 precatalyst, although this system exhibited reasonable catalyst-transfer process during small molecule model

reactions (Table 2, entry 5). Moreover, the $P(t\text{-Bu})_3$ Pd G3 precatalyst yielded unsatisfactory control (still broad PDI of 1.48) even though well-defined $P(t\text{-Bu})_3\text{-Pd(II)-(}o\text{-tolyl)-I}$ I was employed in the SCTP (Table 2, entry 6). To test the versatility of this new SCTP method using an SPhos or RuPhos Pd G3 precatalyst, we increased the M/I ratio to 50 to acquire a higher molar mass. Unfortunately, both cases afforded P3HT with broad PDI values (1.39 - 1.66) in significantly lower yields (60 - 64%), presumably, due to side reactions such as protodeboronation of **M3** (Table 2, entries 7 and 8).

Generally, Pd-catalyzed Suzuki-Miyaura reactions of heterocyclic boronic acid and boronates are challenging because of the unavoidable undesired protodeboronation, which lowers the yield of the products.^{8h,9,10c,12} Nevertheless, we initially chose heterocyclic **M3**-containing pinacol boronate as a monomer, hoping for successful SCTP, because it was reported that highly active SPhos-Pd(0) and RuPhos-Pd(0) catalysts could significantly facilitate the Suzuki-Miyaura reaction over the undesired competing protodeboronation in small molecule studies.^{8e,8h} However, unsatisfactory results such as broad PDI and low yields (Table 2) clearly indicated that protodeboronation due to the fast release of boronic acid from pinacol-protected **M3**, inevitably disrupted controlled polymerization. Then, it became obvious that suppressing protodeboronation would enhance the controlled SCTP. To realize this, we switched the pinacol boronate monomer (**M3**) to MIDA-protected 5-bromo-4-*n*-hexylthien-2-yl-MIDA-boronate (**M4**) because slow hydrolysis of MIDA boronates under mild basic conditions would definitely maximize the effective [catalyst]/[boronic acid] ratio, thereby favoring the C - C bond coupling reaction over the undesired protodeboronation throughout the polymerization.^{9,10b} Therefore, with this modified strategy, we envisioned improvements on both

polymerization yield and more importantly, polymerization control. To test this idea, the same polymerization, under the previously optimized conditions for **M3** (Table 2, entries 3 and 4), was carried out using **M4** instead (Table 3). Our initial trial using **M4** (M/I = 25) and *in situ*-generated SPhos-Pd(II)-(o-tolyl)-I from SPhos Pd G3 precatalysts and 2-iodotoluene at 50 °C for 1 h in THF/H₂O (0.02 M, v/v = 12/1) produced P3HT with low PDI (1.17) and an isolated yield of 82%, after 72 h at room temperature (Table 3, entry 1). The slow hydrolysis inevitably prolonged the polymerization time, a sharp contrast to the polymerization reaction with **M3**. To speed up the hydrolysis of the MIDA boronate, the reaction temperature was increased to 35 °C and subsequently, to 45 °C. Indeed, the polymerizations were completed within 48 h and 24 h, respectively (Table 3, entries 2 and 3). However, the yield of P3HT was still between 82 and 85%, and PDI from the polymerization at 45 °C was relatively broader than that at 35 °C (1.28 vs. 1.16; Table 3, entries 2 and 3). To further optimize the polymerization process, we switched the catalyst from SPhos Pd G3 to RuPhos Pd G3, and conducted the polymerization in mixed solvents (THF/H₂O(v/v) = 30/1) at a higher temperature (45 °C). This resulted in faster polymerization with shorter reaction times (22 h) and yielded P3HT with excellent PDI control (1.09), high yield (94%), and perfect regioregularity (>99%; Table 3, entry 4 and Figure S1a). Interestingly, polymerization in the absence of 2-iodotoluene under otherwise identical conditions afforded a very low isolated yield of 18%, implying significant protodeboronation of **M4** (Table 3, entry 5). Probably, the absence of 2-iodotoluene significantly slowed down the initiation of the RuPhos Pd G3 precatalyst forming the actual propagating catalyst, RuPhos-Pd(II)-3HT-Br. This slowed down the propagation or catalyst-transfer process but instead facilitated protodeboronation. Hence, we concluded that fast and

Table 3. SCTP of M4 or M5 using L-Pd G3 precatalysts



Entry	M/I	R	Pd catalyst (equiv.)	Ligand (equiv.)	THF/H ₂ O (conc., v/v)	Temperature	Time	M _n (PDI) ^a	Yield ^b
1	25	2-Me	SPhos Pd G3 (0.04)	SPhos (0.04)	0.02 M (12/1)	RT	72 h	9.2k (1.17)	82 %
2	25	2-Me	SPhos Pd G3 (0.04)	SPhos (0.04)	0.02 M (12/1)	35 °C	48 h	8.9k (1.16)	85 %
3	25	2-Me	SPhos Pd G3 (0.04)	SPhos (0.04)	0.02 M (12/1)	45 °C	24 h	9.7k (1.28)	82 %
4	25	2-Me	RuPhos Pd G3 (0.04)	RuPhos (0.06)	0.01 M (30/1)	45 °C	22 h	6.5k (1.09)	94 %
5 ^c	25	2-Me	RuPhos Pd G3 (0.04)	RuPhos (0.06)	0.01 M (30/1)	45 °C	21 h	4.7k (1.26)	18 %
6	15	2-Me	RuPhos Pd G3 (0.067)	RuPhos (0.10)	0.01 M (30/1)	45 °C	15 h	4.7k (1.11)	95 %
7	50	2-Me	RuPhos Pd G3 (0.02)	RuPhos (0.03)	0.01 M (30/1)	45 °C	25 h	12.6k (1.18)	96 %
8	75	2-Me	RuPhos Pd G3 (0.013)	RuPhos (0.02)	0.01 M (30/1)	45 °C	22 h	13.7k (1.44)	97 %
9	75	4-CN	RuPhos Pd G3 (0.013)	RuPhos (0.02)	0.01 M (30/1)	45 °C	15 h	16.7k (1.41)	91 %
10 ^d	75	4-CN	RuPhos Pd G3 (0.013)	RuPhos (0.02)	0.01 M (30/1)	45 °C	15 h	16.6k (1.29)	95 %
11 ^d	100	4-CN	RuPhos Pd G3 (0.01)	RuPhos (0.015)	0.01 M (30/1)	45 °C	15 h	20.0k (1.44)	90 %
12 ^{d, e}	25	4-CN	RuPhos Pd G3 (0.04)	RuPhos (0.06)	0.01 M (30/1)	45 °C	15 h	6.8k (1.10)	96 %
13 ^{d, e}	50	4-CN	RuPhos Pd G3 (0.02)	RuPhos (0.03)	0.01 M (30/1)	45 °C	15 h	11.2k (1.20)	97 %
14 ^{d, e}	75	4-CN	RuPhos Pd G3 (0.013)	RuPhos (0.02)	0.01 M (30/1)	45 °C	15 h	16.1k (1.24)	96 %
15 ^{d, e}	100	4-CN	RuPhos Pd G3 (0.01)	RuPhos (0.015)	0.01 M (30/1)	45 °C	15 h	17.2k (1.37)	91 %

Reaction condition: **M4** (0.2 mmol, 1 equiv.), RuPhos Pd G3, Ar-I (0.95 equiv. relative to the catalyst), ligand, K₃PO₄ (1.2 mmol), THF/H₂O. ^aTHF SEC calibrated using polystyrene standards. ^bIsolated yield. ^cCatalyst was prepared in the absence of 2-iodotoluene. ^dCatalyst was prepared for 15 min. ^e**M5** was used.

efficient formation of the active initiator L-Pd(II)-(o-tolyl)-I, prior to

polymerization, must be essential for successful controlled SCTP.

With the optimized conditions in hand, we next investigated the possibility of controlled polymerization of P3HT by varying the M/I ratio and examining their molecular weights. For M/I values ranging from 15 to 50, the new SCTP polymerization successfully produced P3HT with a narrow PDI (1.09 - 1.18), high yield (>94%), and excellent regioregularity (>99%) (Table 3, entries 4, 6, and 7). Moreover, an excellent linear relationship between $[M4]/[catalyst]$ and M_n values (4.7 - 12.6 kg/mol) was observed (Table 3, entries 4, 6, and 7 and Figure 2a). However, the same polymerization at an M/I value of 75 afforded P3HT with relatively broad PDI (1.44) and a lower M_n (13.7 kg/mol) than the expected value presumably due to catalyst decomposition at higher turnover numbers (Table 3, entry 8). To improve the initiation process, we screened various initiators (Table 3, entry 9 and Table S2, entries 15 - 17), other than 2-iodotoluene, which required an induction period of 1 h for the formation of the active well-defined initiator due to its bulky *ortho*-methyl group. After this screening, we switched the initiator to 4-iodobenzonitrile containing an electron-withdrawing group and proceeded the polymerization at M/I = 75 with the intention of more efficient formation of the active Pd catalyst. We observed increased M_n values (16.7 kg/mol) with moderate PDI (1.41) (Table 3, entry 9). Based on the faster oxidative addition of 4-iodobenzonitrile to L-Pd(0), we reduced the induction period to 15 min and under the otherwise identical conditions, at an M/I value of 75, P3HT with an M_n value of 16.6 kg/mol and a narrow PDI (1.29) was isolated in 95 % yield (Table 3, entry 10). To prepare even higher molecular weight polymers, we further increased the M/I ratio to 100 and produced P3HT with an M_n value of 20.0 kg/mol and moderate PDI (1.44; Table 3, entry 11). As a result, we overall achieved excellent controlled SCTP with linearly increased M_n (4.7 -

20.0 kg/mol), narrow PDI (1.09 - 1.44), high yield (>90%), and high regioregularity (>99%) over a wide range of M/I ratios (15 - 100) (Table 3, entries 4, 6, 7, 10, and 11, Figure 2a, and Table S2, entries 18 and 19). We also measured absolute molecular weights of P3HT by multi-angle laser light scattering (MALLS) and found that the results were consistent with theoretical molecular weights with narrow PDI values of 1.06 - 1.16 (DP = 25 - 100, Figure 2). In addition to the P3HT results, using the same protocol, polymerization of the more sterically demanding 5-bromo-4-(2'-ethylhexyl)thien-2-yl-MIDA-boronate (**M5**), also proceeded well with excellent control to produce with DP ranging from 25 to 100 poly(3-(2'-ethylhexyl)thiophene) (P3EHT), narrow PDI (1.10 - 1.37), high yield (>91%), and high regioregularity (>99%) (Table 3, entries 12 - 15).

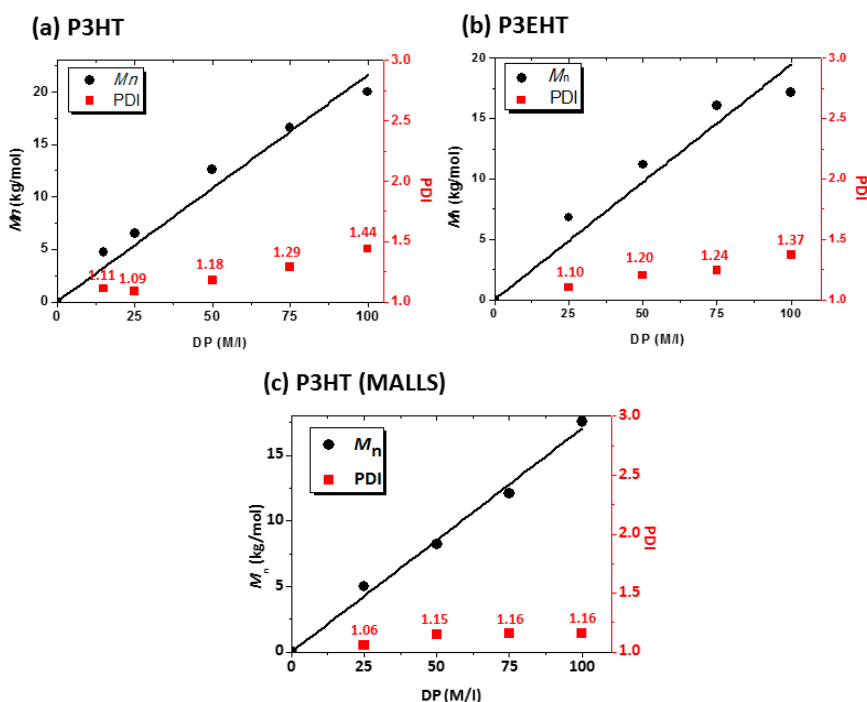


Figure 2. Plot of M_n versus M/I for (a) P3HT-RI, (b) P3EHT-RI, and (c) P3HT-MALLS prepared by SCTP using **M4**, **M5**, and RuPhos Pd G3 precatalysts in their optimal conditions.

A key factor to a successful SCTP was the efficient formation of the actual initiator, the well-defined Buchwald L-Pd(II)-aryl-I, from L-Pd G3 precatalysts and aryl iodides. Therefore, we assumed that detailed investigation of this initiation process would provide a better understanding of the

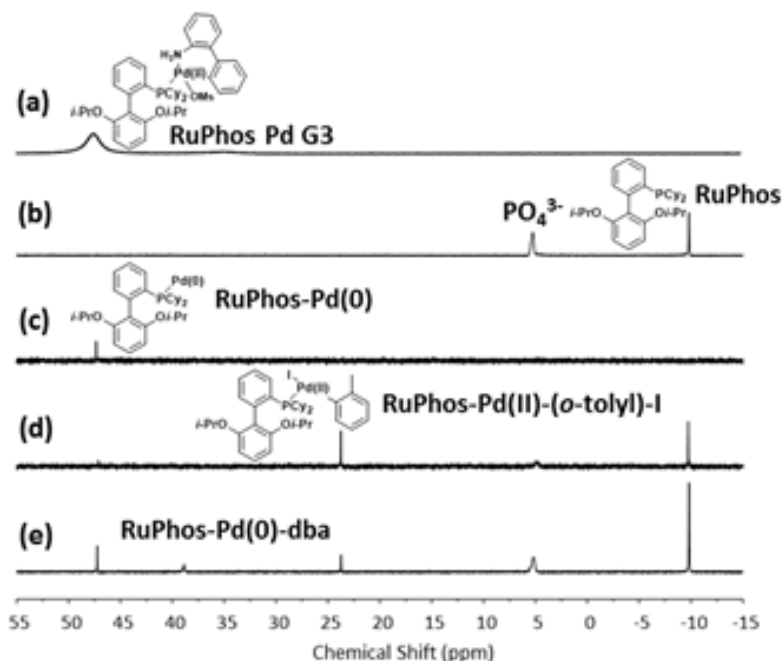


Figure 3. ^{31}P NMR spectra of (a) initial RuPhos Pd G3, (b) RuPhos + K_3PO_4 (c) RuPhos Pd G3 + K_3PO_4 , (d) RuPhos Pd G3 + RuPhos + 2-iodotoluene + K_3PO_4 , and (e) Pd_2dba_3 +RuPhos+2-iodotoluene+ K_3PO_4 in $\text{THF-d}_8/\text{D}_2\text{O}$ ($v/v=4/1$) at 50 °C for 1 h.

controlled SCTP. We monitored catalytic complex formation during initiation with ^{31}P NMR spectroscopy because various catalytic complexes could be easily identified from their distinct chemical shifts. Firstly, the RuPhos Pd G3 precatalyst, displayed as a broad signal at 47.4 ppm (Figure 3a), was treated with 6 equiv. of K_3PO_4 at 50 °C in $\text{THF-d}_8/\text{D}_2\text{O}$ for 1 h. The ^{31}P NMR spectrum of the resultant reaction

mixture revealed a new sharp peak at 47.2 ppm corresponding to RuPhos-Pd(0), with the complete consumption of the precatalyst (Figure 3c). This result is consistent with previous literature that demonstrated the exclusive formation of RuPhos-Pd(0) from RuPhos Pd G3 precatalysts under mild basic conditions.⁸ⁱ Next, to directly identify the externally initiated catalyst or the actual initiator of the polymerization, we carried out the same process in the presence of 1 equiv. of 2-iodotoluene and 1.5 equiv. of additional RuPhos ligands. The ³¹P NMR spectrum of the crude reaction mixture displayed other new peaks at 23.7 ppm and -9.7 ppm corresponding to RuPhos-Pd(II)-(o-tolyl)-I and the additional RuPhos ligand, respectively (Figure 3d). Overall, these results indicated that a fast and high yielding transformation from the RuPhos Pd G3 precatalyst to the actual RuPhos-Pd(II)-(o-tolyl)-I initiator via a RuPhos-Pd(0) intermediate occurred efficiently under mild conditions. On the other hand, an attempt to prepare RuPhos-Pd(II)-(o-tolyl)-I directly from Pd₂dba₃, RuPhos, and 2-iodotoluene under the same conditions was less successful. This reaction generated a mixture of three different catalytic complexes comprising RuPhos-Pd(0), RuPhos-Pd(II)-(o-tolyl)-I, and another complex tentatively assigned as RuPhos-Pd(0)-dba (38.8 ppm) (Figure 3e). Because of this inefficient initiation, P3HT produced from Pd₂dba₃ resulted in a broad PDI with less control (Table 2, entry 1). Thus, we concluded that using L-Pd G3 precatalysts as a well-defined L-Pd(0) source was the key to the exclusive formation of the externally initiated L-Pd(II)-aryl-I, thereby leading to controlled SCTP. Furthermore, the *in situ* preparation protocol was user-friendly because L-Pd G3 precatalysts were bench-stable solids, easy to handle, and commercially available (Figure 1d). Moreover, a wide range of aryl iodides could be used to form the externally initiated catalysts (Figure 1d), introducing various functional

groups to one of the polymer chain-ends.

To further confirm chain-growth polymerization, we examined chain-end fidelity of P3HT using matrix-assisted laser desorption/ionization time-of-flight (MALDI-TOF) mass spectrometry. The MALDI-TOF spectrum of P3HT, prepared from pinacol-based **M3** (major) and *o*-tolyl/Br (minor) chain-ends (Figure 4a). This suggested that competing chain-transfer reactions occurred during SCTP. In contrast, the MALDI-TOF spectrum of P3HT prepared from MIDA-based **M4** clearly displayed only a clean single distribution of peaks corresponding to the desired P3HT with *o*-tolyl/H chain-ends (Figure 4b). This confirmed that SCTP using **M4** was free from any chain-transfer reaction, thereby leading to better-controlled polymerization with higher chain-end fidelity than those observed for **M3**.

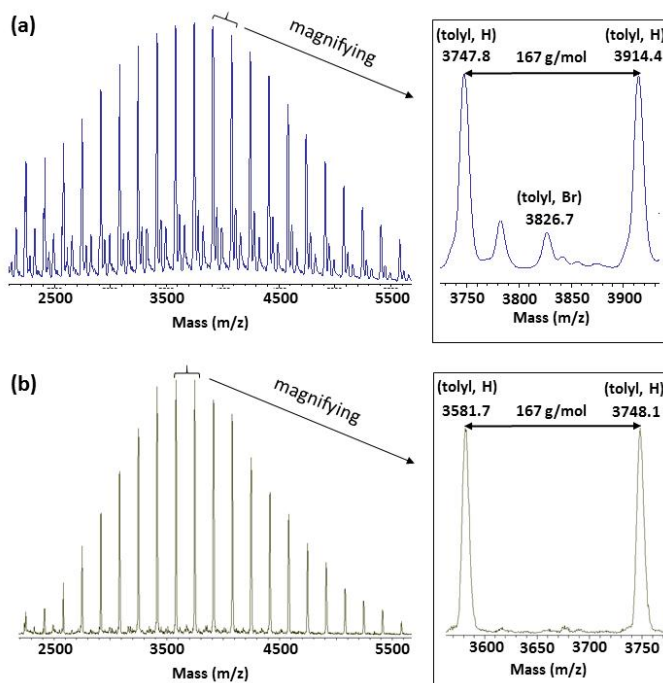


Figure 4. MALDI-TOF spectra of P3HT prepared by SCTP of (a) **M3** ($M/I = 25$; Table 2, entry 4) and (b) **M4** ($M/I = 25$; Table 3, entry 4).

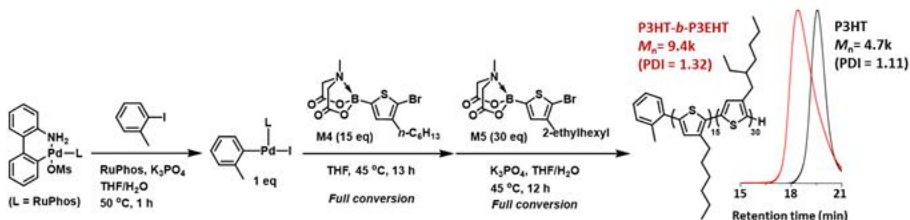


Figure 5. Synthesis of P3HT-*b*-P3EHT by SCTP using **M4** and **M5** with RuPhos Pd G3 precatalyst

One of the essential criteria for controlled chain-growth polymerization is the retention of living chain-ends, thereby allowing for successful chain extension and block copolymerization from the macroinitiator of the homopolymer. Notably, to date, the block copolymerization of two different thiophene monomers using the previous SCTP has been nearly impossible.¹¹ Therefore, we carried out the block copolymerization of P3HT-*b*-P3EHT to highlight the power of this much-improved controlled SCTP protocol for synthesis of P3AT derivatives. Firstly, a macroinitiator of P3HT, the first block ($M_n = 4.7$ k and PDI = 1.11), was prepared with DP of 15, using our optimized conditions with **M4** and RuPhos Pd G3 precatalysts (Table 3, entry 6 and Figure 5). Next, to the same reaction pot, **M5** was added to produce P3HT-*b*-P3EHT ($[\mathbf{M5}]/[\text{macroinitiator}] = 30/1$) (Figure 5). Indeed, the SEC trace of the P3HT macroinitiator clearly shifted to a higher molecular weight ($M_n = 7.5$ k and PDI = 1.35; Figure 5). Additionally, the ¹H NMR spectrum of the resulting block polymer displayed two methylene peaks at 2.73 ppm and 2.80 ppm corresponding to P3EHT and P3HT, respectively (Supporting Information). This confirmed successful block copolymerization using strategies with RuPhos Pd G3 precatalysts and MIDA-boronates.

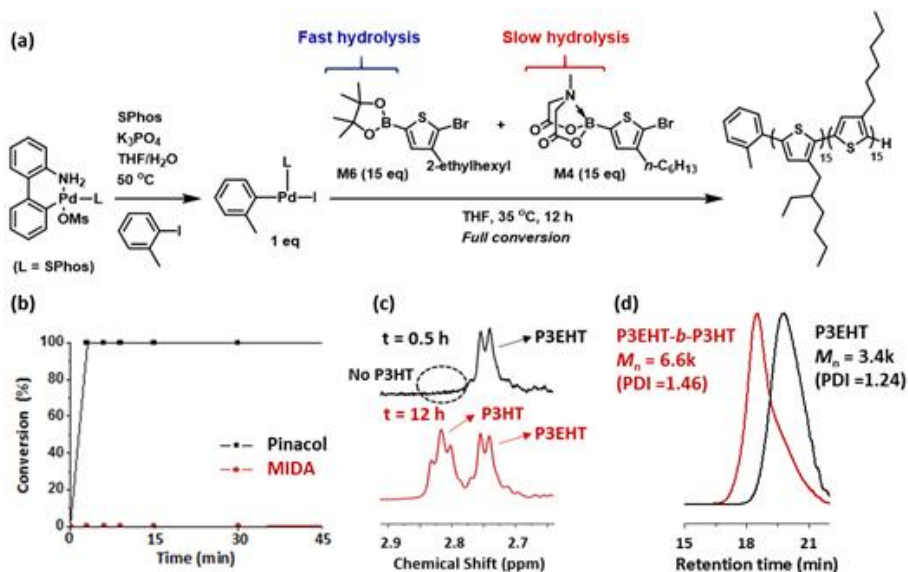


Figure 6. (a) One-shot preparation of P3EHT-*b*-P3HT by SCTP using **M4**, **M6**, and SPhos Pd G3 precatalyst. (b) Conversion vs. time plot of protecting groups of **M4** and **M6** in one-shot SCTP block copolymerization. (c) ^1H NMR analysis on the one-shot polymerization of P3EHT-*b*-P3HT. (d) SEC traces of one-shot SCTP block copolymerization.

With this successful block copolymerization by the sequential addition of **M4** and **M5**, we carried out a simpler but more challenging one-shot copolymerization by the simultaneous addition of two monomers to prepare the P3EHT-*b*-P3HT (Figure 6). One-shot block copolymerization is extremely challenging and requires two monomers with very different reactivities.^{14e} For example, one-shot block copolymerization using KCTP has been virtually impossible due to the similar reactivity of the Grignard monomers.^{6d} Previously, such an attempt was made by adding lithium chloride to a mixture of two thiophene Grignard regioisomers.¹³ Unfortunately, this resulted in uncontrolled block copolymerization, displaying a bimodal SEC trace and defects in regioregularity.¹³ In contrast, we envisioned that

one-shot copolymerization using this new SCTP could be possible if one cleverly utilizes the vastly different hydrolysis rates between pinacol boronates and MIDA boronates without compromising regioregularity as well as the polymerization initiation rate of the second block (Figure 6). To perform one-shot block copolymerization, a mixture of MIDA-based **M4** and 5-bromo-4-(2'-ethylhexyl) thien-2-yl-pinacol-boronate (**M6**) in THF was immediately added to *in situ*-generated SPhos-Pd(II)-(o-tolyl)-I from Buchwald SPhos Pd G3 precatalysts; the resulting mixture was stirred at 35 °C for 12 h (Figure 6a). Time-dependent ¹H NMR monitoring of the crude copolymerization mixture revealed that the more reactive pinacol boronate **M6** was completely converted to P3EHT within 30 min due to fast release to the corresponding boronic acids (Figures 6b, c and 7). Subsequently, polymerization of the MIDA-protected **M4** began to occur

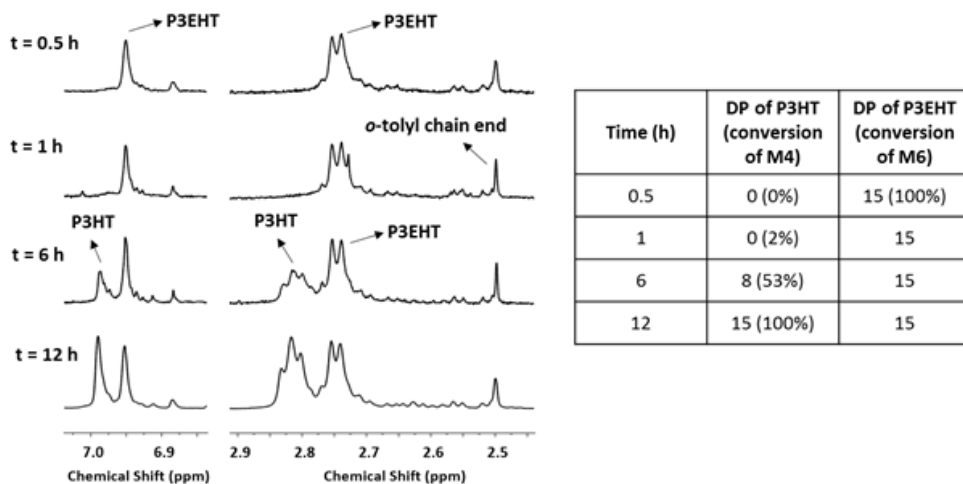


Figure 7. ¹H NMR analysis on the one-shot polymerization of P3EHT₁₅-*b*-P3HT₁₅

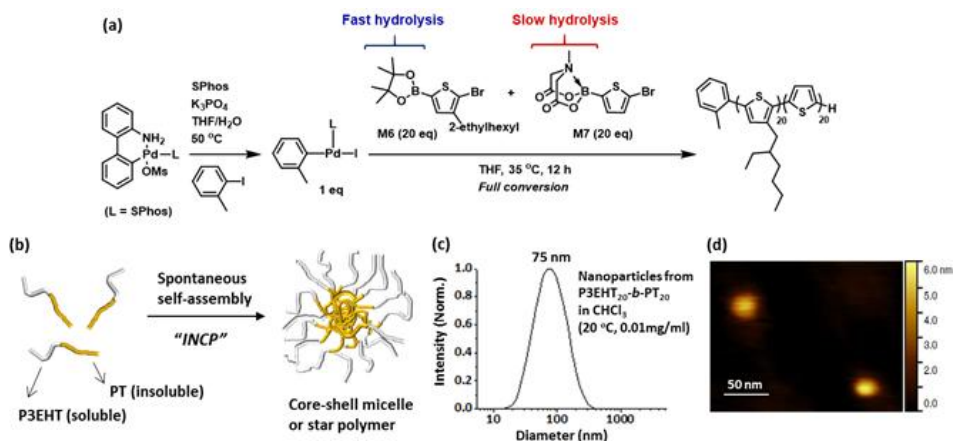


Figure 8. (a) One-shot preparation of P3EHT-*b*-PT by SFTP using **M6**, **M7**, and SPhos Pd G3 precatalyst. (b) INCP process of P3EHT-*b*-PT into core-shell micelles and star polymer nanoparticles. (c) DLS analysis and (d) AFM image of nanoparticles prepared by the one-shot copolymerization (20 °C, 0.01 mg/mL).

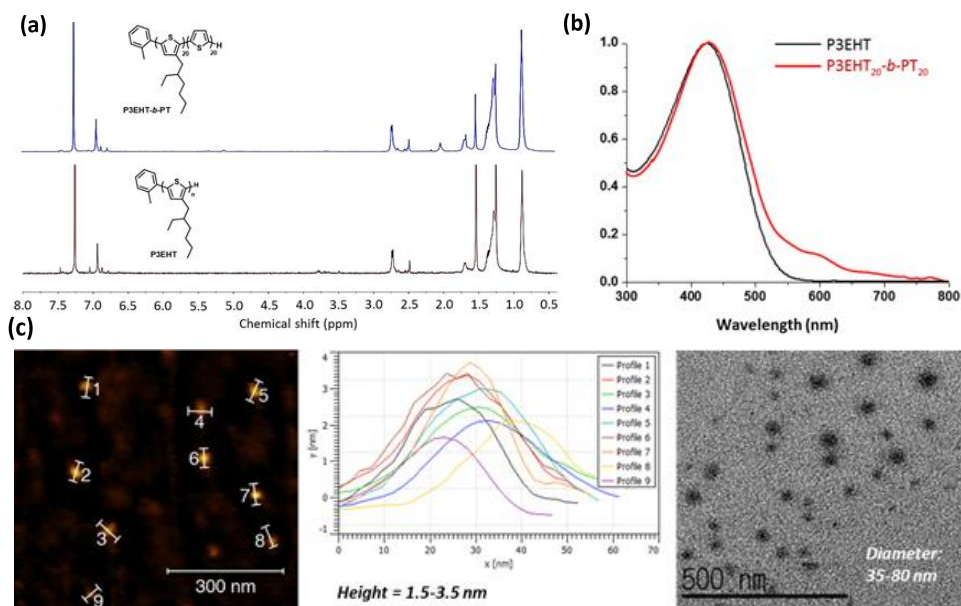


Figure 9. (a) ^1H NMR spectra of P3EHT and P3EHT₂₀-*b*-PT₂₀ (CDCl_3), (b) UV-vis spectra of nanoparticles from P3EHT₂₀-*b*-PT₂₀, and (c) AFM and TEM images of nanoparticles from P3EHT₂₀-*b*-PT₂₀

slowly after 1 h (Figure 7). Moreover, the SEC trace measured after 30 min (corresponding to P3EHT, $M_n = 3.4k$ and PDI = 1.24) clearly shifted to a higher molecular weight ($M_n = 6.6k$ and PDI = 1.46) after 12 h, suggesting a successful chain extension, thereby producing P3EHT-*b*-P3HT by one-shot copolymerization (Figure 6d).

To further demonstrate the synthetic utility of this one-shot block copolymerization, we attempted the one-shot *in situ* nanoparticlization of conjugated polymers (INCP), a step-economic and direct self-assembly method for spontaneous formation of nanoparticles made of conjugated polymers.¹⁴ The main driving forces for this *in situ* nanoparticlization are insolubility and strong p-p interactions of the second conjugated blocks, such as polythiophenes (PT), without any side chains.^{14c, d, g} As a result, the insoluble second block undergoes spontaneous self-assembly during polymerization, eventually forming core-shell-type micelles (Figure 8b). For example, *in situ* nanoparticlization of P3EHT-*b*-PT and P3HT-*b*-PT prepared by sequential addition of the two monomers via KCTP generated linear and branched nanostructures in a hierarchical manner.^{14c, g} Now, with a one-shot block copolymerization strategy by the SCTP method, one should be able to prepare nanoparticles consisting of polythiophenes via one-shot INCP where block copolymerization and *in situ* self-assembly process would occur simultaneously.^{14c} This would provide the most step-economic protocol for nanoparticlization of conjugated polymers. To perform one-shot INCP, we added a mixture of monomers, **M6**, and 5-bromothiophen-2-yl-MIDA-boronate (**M7**) to a reaction flask containing SPhos-Pd(II)-(o-tolyl)-I, in one go; the mixture was then stirred at 35 °C for 12 h (Figure 8a). Similar to our previous reports on INCP, initial evidences of the successful one-shot *in situ* nanoparticlization of P3EHT-*b*-PT came from ¹H NMR and UV-vis spectroscopy.^{14c} The ¹H NMR spectrum of the resulting polymer

displayed peaks that exactly matched those of P3EHT (Figure 9a). This occurred because the PT blocks forming the core of the micelles were not solvated by CDCl_3 and hence, were undetected (Figure 9).^{14c} UV-vis spectra of the resulting polymers exhibited absorption at 250 - 640 nm with distinct vibronic peaks at 544 and 590 nm, corresponding to p-p interactions of the aggregated PT blocks, even in chloroform solution (Figure 9b).^{14c} Subsequently, information on the size and morphology of the P3EHT-*b*-PT nanoparticles were characterized by dynamic light scattering (DLS), atomic force microscopy (AFM), and transmission electron microscopy (TEM) techniques. DLS measurements at 20 °C indicated an average hydrodynamic diameter for nanoparticles of 75 nm in chloroform solution (Figure 8c). From two independent visualizations of AFM images on highly ordered pyrolytic graphite (HOPG) and TEM images on a copper/carbon grid, P3EHT-*b*-PT nanoparticles clearly displayed a semi-conducting star polymer or spherical nanoparticles with a height of 5 nm (Figures 8d and 9c).

Conclusions

In conclusion, we developed significantly improved strategies for SCTP with a much better controlled polymerization of 3-alkylthiophenes using fast initiating bench-stable Buchwald RuPhos (and SPhos) Pd G3 precatalysts and slow-releasing MIDA-protected boronates. Optimizing model reactions with small molecules revealed that RuPhos (and SPhos) Pd G3 precatalysts were the best catalysts for the catalyst-transfer reactions. For controlled SCTP, the RuPhos Pd G3 precatalyst promoted the rapid formation of well-defined externally initiated catalysts that were the key for a successful controlled polymerization. Moreover, use of MIDA-boronates instead of pinacol boronates, effectively suppressed side reactions such as chain-transfers and protodeboronation, resulting in greatly improved controlled polymerization to afford high molecular weight and defect-free P3ATs in excellent yield. Thus, this new SCTP method provided a solution to overcome previous limitations such as air-sensitivity of catalysts, protodeboronation of monomers, and loss of polymerization control. Furthermore, advantages of the new controlled SCTP protocol were highlighted by the first successful demonstration of block copolymerization of two thiophene monomers, one-shot block copolymerization, and even one-shot INCP to produce semi-conducting star polymer nanoparticles consisting of polythiophenes. We believe that this new protocol makes SCTP an excellent alternative to the current KCTP method and this would certainly expand its utility toward the controlled synthesis of novel conjugated polymers and their semi-conducting nanostructures.

References

(1) (a) Brabec, C. J.; Gowrisanker, S.; Halls, J. J. M.; Laird, D.; Jia, S.; Williams, S. P. *Adv. Mater.* 2010, *22*, 3839–3856. (b) Beaujuge, P. M.; Fréchet, J. M. J. *J. Am. Chem. Soc.* 2011, *133*, 20009–20029. (c) Boudreault, P.-L. T.; Najari, A.; Leclerc, M. *Chem. Mater.* 2011, *23*, 456–469. (d) Facchetti, A. *Chem. Mater.* 2011, *23*, 733–758. (e) Li, G.; Zhu, R.; Yang, Y. *Nat. Photonics* 2012, *6*, 153–161. (f) Yeh, N.; Yeh, P. *Renewable Sustainable Energy Rev.* 2013, *21*, 421–431. (g) Cataldo, S.; Pignataro, B. *Materials* 2013, *6*, 1159–1190.

(2) (a) Kline, R. J.; McGehee, M. D.; Kadnikova, E. N.; Liu, J.; Fréchet, J. M. J. *Adv. Mater.* 2003, *15*, 1519–1522. (b) Goh, C.; Kline, R. J.; McGehee, M. D.; Kadnikova, E. N.; Fréchet, J. M. J. *Appl. Phys. Lett.* 2005, *86*, 122110. (c) Kim, Y.; Cook, S.; Tuladhar, S. M.; Choulis, S. A.; Nelson, J.; Durrant, J. R.; Bradley, D. D. C.; Giles, M.; McCulloch, I.; Ha, C.-S.; Ree, M. *Nature Mater.* 2006, *5*, 197–203. (d) Gunes, S.; Neugebauer, H.; Sariciftci, N. S. *Chem. Rev.* 2007, *107*, 1324–1338. (e) Marrocchi, A.; Lanari, D.; Facchetti, A.; Vaccaro, L. *Energy Environ. Sci.* 2012, *5*, 8457–8474. (f) Persson, N. E.; Chu, P.-H.; McBride, M.; Grover, M.; Reichmanis, E. *Acc. Chem. Res.* 2017, *50*, 932–942.

(3) (a) Cheng, Y.-J.; Yang, S.-H.; Hsu, C.-S. *Chem. Rev.* 2009, *109*, 5868–5923. (b) Sakamoto, J.; Rehahn, M.; Wegner, G.; Schlüter, A. D. *Macromol. Rapid Commun.* 2009, *30*, 653–687. (c) Carsten, B.; He, F.; Son, H. J.; Xu, T.; Yu, L. *Chem. Rev.* 2011, *111*, 1493–1528.

(4) (a) Yokoyama, A.; Yokozawa, T. *Macromolecules* 2007, *40*, 4093–4101. (b) Osaka, I.; McCullough, R. D. *Acc. Chem. Res.* 2008, *41*, 1202–1214. (c) Miyakoshi, R.; Yokoyama, A.; Yokozawa, T. *J. Polym. Sci., Polym. Chem.* 2008, *46*, 753–765. (d) Yokozawa, T.; Yokoyama, A. *Chem. Rev.* 2009, *109*, 5595–5619. (e) Geng, Y.; Huang, L.; Wu, S.; Wang, F. *Sci. China Chem.* 2010, *53*, 1620–1633. (f) Kiriy, A.; Senkovskyy, V.; Sommer, M. *Macromol. Rapid Commun.* 2011, *32*, 1503–1517. (g) Okamoto, K.; Luscombe, C. K. *Polym. Chem.* 2011, *2*, 2424–2434. (h) Yokozawa, T.; Nanashima, Y.; Ohta, Y. *ACS Macro Lett.* 2012, *1*, 862–866. (i) Stefan, M. C.; Bhatt, M. P.; Sista, P.; Magurudeniya, H. D. *Polym. Chem.* 2012, *3*, 1693–1701. (j) Bryan, Z. J.; McNeil, A. J. *Macromolecules* 2013, *46*, 8395–8405. (k) Kang, S.; Ono, R. J.; Bielawski, C. W. *J. Am. Chem. Soc.* 2013, *135*, 4984–4987. (l) Qiu, Y.; Mohin, J.; Tsai, C.-H.; Tristram-Nagle, S.; Gil, R. R.; Kowalewski, T.; Noonan, K. J. T. *Macromol. Rapid Commun.* 2015, *36*, 840–844. (m) Yokozawa, T. Ohta, Y.

Chem. Rev., 2016, *116*, 1950–1968. (n) Verheyen, L.; Leysen, P.; Eede, M.-P. V. D.; Ceunen, W.; Hardeman, T.; Koeckelberghs, G. *Polymer* 2017, *108*, 521–546.

(5) (a) Yokoyama, A.; Miyakoshi, R.; Yokozawa, T. *Macromolecules* 2004, *37*, 1169–1171. (b) Miyakoshi, R.; Yokoyama, A.; Yokozawa, T. *Macromol. Rapid Commun.* 2004, *25*, 1663–1666. (c) Sheina, E. E.; Liu, J. S.; Iovu, M. C.; Laird, D. W.; McCullough, R. D. *Macromolecules* 2004, *37*, 3526–3528. (d) Miyakoshi, R.; Yokoyama, A.; Yokozawa, T. *J. Am. Chem. Soc.* 2005, *127*, 17542–17547. (e) Zhang, Y.; Tajima, K.; Hirota, K.; Hashimoto, K. *J. Am. Chem. Soc.* 2008, *130*, 7812–7813. (f) Hollinger, J.; Jahnke, A. A.; Coombs, N.; Seferos, D. S. *J. Am. Chem. Soc.* 2010, *132*, 8546–8547.

(6) (a) Bronstein, H. A.; Luscombe, C. K. *J. Am. Chem. Soc.* 2009, *132*, 12894–12895. (b) Smeets, A.; VandenBergh, K.; DeWinter, J.; Gerbaux, P.; Verbiest, T.; Koeckelberghs, G. *Macromolecules* 2009, *42*, 7638–7641. (c) Tkachov, R.; Senkovskyy, V.; Komber, H.; Sommer, J.-U.; Kiriy, A. *J. Am. Chem. Soc.* 2010, *132*, 7803–7810. (d) Palermo, E. F.; McNeil, A. J. *Macromolecules* 2012, *45*, 5948–5955. (e) Chavez, C. A.; Choi, J.; Nesterov, E. E. *Macromolecules* 2014, *47*, 506–516.

(7) (a) Yokoyama, A.; Suzuki, H.; Kubota, Y.; Ohuchi, K.; Higashimura, H.; Yokozawa, T. *J. Am. Chem. Soc.* 2007, *129*, 7236–7237. (b) Zhang, H.-H.; Xing, C.-H.; Hu, Q.-S. *J. Am. Chem. Soc.* 2012, *134*, 13156–13159. (c) Zhang, H.-H.; Xing, C.-H.; Hu, Q.-S.; Hong, K. *Macromolecules* 2015, *48*, 967–978. (d) Nojima, M.; Ohta, Y.; Yokozawa, T. *J. Am. Chem. Soc.* 2015, *137*, 5682–5685. (e) Zhang, H.-H.; Peng, W.; Dong, J.; Hu, Q.-S. *ACS Macro Letters* 2016, *5*, 656–660. (f) Qiu, T.; Worch, J. C.; Fortney, A.; Gayathri, C.; Gil, R. T.; Noonan, K. J. T. *Macromolecules* 2016, *49*, 4757–4762. (g) Zhang, H.-H.; Ma, C.; Bonnesen, P. V.; Zhu, J.; Sumpter, B. G.; Carrillo, J.-M. Y.; Yin, P.; Wang, Y.; Li, A.-P.; Hong, K. *Macromolecules* 2016, *49*, 4691–4698.

(8) (a) Miyaura, N.; Yamada, K.; Suzuki, A. *Tetrahedron Lett.* 1979, *36*, 3427–3430. (b) Miyaura, N.; Suzuki, A. *Chem. Rev.* 1995, *95*, 2457–2483. (c) Miyaura, N. *J. Organomet. Chem.* 2002, *653*, 54–57. (d) Tyrell, E.; Brookes, P. *Synthesis* 2003, 469–483. (e) Billingsley, K. L.; Anderson, K. W.; Buchwald, S. L. *Angew. Chem., Int. Ed.* 2006, *45*, 3484–3488. (f) Billingsley, K. L.; Buchwald, S. L. *J. Am. Chem. Soc.* 2007, *129*, 3358–3366. (g) Martin, R.; Buchwald, S. L. *Acc. Chem. Res.* 2008, *41*, 1461–1473. (h) Kinzel, T.; Zhang, Y.; Buchwald, S. L. *J. Am. Chem. Soc.* 2010, *132*, 14073–14075. (i) Bruno, N. C.; Tudge, M. T.; Buchwald, S. L. *Chem. Sci.* 2013, *4*, 916–920. (j) Suzuki, A. *Angew. Chem., Int. Ed.* 2011, *50*, 6722–6737. (k) Lennox, A. J. J.; Lloyd-Jones, G. C. *Chem. Soc. Rev.* 2014, *43*, 412–443.

(9) (a) Gillis, E. P.; Burke, M. D. *J. Am. Chem. Soc.* 2007, *129*, 6716–6717. (b) Lee, S. J.; Gray, K. C.; Paek, J. S.; Burke, M. D. *J. Am. Chem. Soc.* 2008, *130*, 466–468. (c) Knapp, D. M.; Gillis, E. P.; Burke, M. D. *J. Am. Chem. Soc.* 2009, *131*, 6961–6963. (d) Li, J.; Ballmer, S. G.; Gillis, E. P.; Fujii, S.; Schmidt, M. J.; Palazzolo, A. M. E.; Lehmann, J. W.; Morehouse, G. F.; Burke, M. D. *Science* 2015, *347*, 1221–1226.

(10) (a) Liu, M.; Chen, Y.; Zhang, C.; Li, C.; Li, W.; Bo, Z. *Polym. Chem.* 2013, *4*, 895–899. (b) Carrillo, J. A.; Ingleson, M. J.; Turner, M. L. *Macromolecules* 2015, *48*, 979–986. (c) Carrillo, J. A.; Turner, M. L.; Ingleson, M. J. *J. Am. Chem. Soc.* 2016, *138*, 13361–13368. (d) Nojima, M.; Kosaka, K.; Kato, M.; Ohta, Y.; Yokozawa, T. *Macromol. Rapid Commun.* 2016, *37*, 79–85. (e) Sugita, H.; Nojima, M.; Ohta, Y.; Yokozawa, T. *Chem. Commun.* 2017, *53*, 396–399.

(11) (a) Yokozawa, T.; Suzuki, R.; Nojima, M.; Ohta, Y.; Yokoyama, A. *Macromol. Rapid Commun.* 2011, *32*, 801–806. (b) Sui, A.; Shi, X.; Tian, H.; Geng, Y.; Wang, F. *Polym. Chem.* 2014, *5*, 7072–7080. (c) Kosaka, K.; Ohta, Y.; Yokozawa, T. *Macromol. Rapid Commun.* 2015, *36*, 373–377.

(12) Cox, P. A.; Leach, A. G.; Campbell, A. D.; Lloyd-Jones, G. C. *J. Am. Chem. Soc.* 2016, *138*, 9145–9157.

(13) Wu, S.; Huang, L.; Tian, H.; Geng, Y.; Wang, F. *Macromolecules* 2011, *44*, 7558–7567.

(14) (a) Yoon, K.-Y.; Lee, I.-H.; Kim, K.O.; Jang, J.; Lee, E.; Choi, T.-L. *J. Am. Chem. Soc.* 2012, *134*, 14291–14294. (b) Kim, J.; Kang, E.-H.; Choi, T.-L. *ACS Macro Letters* 2012, *1*, 1090–1093. (c) Lee, I.-H.; Amaladass, P.; Yoon, K.-Y.; Shin, S.; Kim, Y.-J.; Kim, I.; Lee, E.; Choi, T.-L. *J. Am. Chem. Soc.* 2013, *135*, 17695–17698. (d) Lee, I.-H.; Amaladass, P.; Choi, T.-L. *Chem. Commun.* 2014, *50*, 7945–7948. (e) Shin, S.; Yoon, K.-Y.; Choi, T.-L. *Macromolecules* 2015, *48*, 1390–1397. (f) Lee, I.-H.; Amaladass, P.; Choi, I.; Bergmann, V. W.; Weber, S. A. L.; Choi, T.-L. *Polym. Chem.* 2016, *7*, 1422–1428. (g) Lee, I.-H.; Choi, T.-L. *Polym. Chem.* 2016, *7*, 7135–7141. (h) Yang, S.; Shin, S.; Choi, I.; Lee, J.; Choi, T.-L. *J. Am. Chem. Soc.* 2017, *139*, 3082–3088.

MIDA와 Buchwald 촉매를 이용한 새로운 SCTP 폴리싸이오펜 합성법 개발 및 응용 연구

서 경 배
화학부 유기화학전공
서울대학교 대학원

기존의 Suzuki-Miyaura catalyst transfer polycondensation (SCTP)는 촉매의 air-sensitivity와 낮은 조절 능력, 그리고 boronic acid 단량체의 protodeboronation으로 인해 P3AT 합성에 한계를 갖고 있었다. 따라서 이를 극복하고자 air-stable Buchwald Pd G3 precatalyst 와 MIDA-boronate 전략을 사용하였고, 기존의 한계를 뛰어 넘는 높은 고분자 조절 능력과 yield로 P3AT 를 합성할 수 있었다.

가장먼저 small molecule study를 통해 SPhos-Pd과 RuPhos-Pd 조합의 높은 catalyst-transfer 능력을 알아냈고 additional ligand와 dilute condition을 통해 이를 극대화 할 수 있었다. 또한 air-stable Buchwald Pd G3 precatalyst를 활용한 well-defined external initiator의 효율적 형성을 통해 fast initiation을 달성 하여 polymerization의 control을 높일 수 있었다. 더 나아가 기존의 pinacol-boronate의 protodeboronation을 억제하고자 MIDA-boronate ester를 이용하였으며 이를 통해 부 반응을 억제하고 >90 % yield로 P3AT를 얻을 수 있었다.

최종적으로 새로운 SCTP합성법을 이용하여 기존의 방식으로는 달성하기 어려웠던 fully conjugated thiophene block copolymer을 합성할 수 있었다. 또한 pinacol-boronate와 MIDA-boronate의 hydrolysis 속도 차이를 이용한 one-shot block copolymerization 을 성공적으로 달성 할 수 있었고, 이를 *in situ* generated nanoparticlization으로 확장하여 semiconducting star polymer의 형성을 유도할 수 있었다.

주요어: Suzuki-Miyaura catalyst-transfer polycondensation, Poly(3-alkylthiophene), Buchwald precatalyst, MIDA-boronates, One-shot polymerization, *In situ* nanoparticlization of conjugated polymer.

학번: 2015-20384